

High Pressure Visualisation of Liquid Oxygen and Cryogenic Hydrogen Combustion under an Imposed Acoustic Field

S. Webster¹, J. Hardi¹ and M. Oswald¹

¹Institute of space propulsion, German aerospace agency (DLR),
Lampoldshausen, Baden-Württemberg 74239, Germany

Abstract

Experimental investigations into combustion instability were undertaken using a rectangular subscale combustion chamber. High speed optical diagnostics were used to observe flame-acoustic interactions. A sector wheel was used to produce an acoustic field with time varying amplitude. The acoustic field under investigation is the first transverse mode with a velocity anti node located in the central combustion zone under observation by high speed optical diagnostics. Increased combustion product emission was observed near the face plate for periods of high amplitude excitation. Combustion zones with high emission were convected downstream as excitation amplitudes decreased. During phases of increasing amplitude an increase in emission intensity at the mixing border between dense oxygen and cryogenic hydrogen was observed. This provides visual confirmation of increased mixing efficiency due to high amplitude transverse velocities in the vicinity of the injection plane.

Introduction

Spontaneous thermo-acoustic instability in liquid propellant rocket engines, often referred to as high frequency combustion instability, can lead to the catastrophic end of a launch mission. Avoiding instability has historically been achieved by a costly process of trial and error in engine development. In the hopes of improving predictive capabilities, concurrent experimental and numerical investigations of combustion instability are underway at the German Aerospace Center (DLR), Institute of Space Propulsion, at Lampoldshausen. One experiment is designed to facilitate the study of flame-acoustic interaction, in order to better understand the phenomenology of energy feedback mechanisms which drive self-sustaining instability. This paper reports recent results of testing with high-speed optical diagnostics to characterise the flow field response to acoustic forcing.

The success of predictive models for combustion instability in rockets has historically been limited due to a lag in physical understanding of the behaviour of cryogenic spray flames under the influence of high amplitude acoustic perturbations [5], [11]. In recent years, experimental rocket combustors have been developed which have the ability to simulate the conditions of combustion instability in order to study the flame behaviour [1,2,7,8]. Acoustic fields are forced by exhaust flow modulation and the response of the spray flame studied via large optical access windows.

Conventional diagnostic imaging techniques are applied, for example CH* or OH* chemiluminescence to determine the structure of the reaction zone [3], [6], and backlit shadowgraph imaging to observe the breakup and mixing of the dense cryogenic jets [4]. Acquiring images with high repetition rates allows the dynamic response to be studied, allowing, for example, the time delay of combustion fluctuations to be determined [2], [9]. Such imaging provides both valuable

information to improve understanding of flame-acoustic coupling, and rare data sets for validation of numerical modelling.

By concentrating on different parts of the spectrum, OH* and shadowgraph imaging allow combustion and spray structures to be studied separately. Imaging of the visible spectrum produces a hybrid image, combining qualities of dense phase imaging and combustion emission imaging. In the study of rocket combustion instability, it has so far only been applied with low speed, as a secondary diagnostic [6]. In the current work at DLR Lampoldshausen, high-speed visible imaging has been applied for the first time to resolve acoustic-flame coupling.

This work presents initial findings from the analysis of visible imaging of rocket flames under cycling acoustic forcing. This type of imaging is found to be particularly valuable in the study of flame response to cyclic forcing of the acoustic field, where the dynamic phenomena are defined by alternating periods of acoustic growth and decay. Results from visible imaging are compared to those from OH* imaging collected in parallel.

Method

Experiments were conducted on the European High Pressure Research and Technology Test Facility for cryogenic rocket engines (P8) at DLR Lampoldshausen. The experiments were carried out using the sub scale combustion chamber designated 'BKH', illustrated in figure 1. BKH is a rectangular combustion chamber designed to investigate acoustic-combustion interaction. Five shear coaxial injection elements are clustered in the centre of the head end of the chamber. These elements inject a central jet of [10]liquid oxygen surrounded by an annulus of high velocity hydrogen.

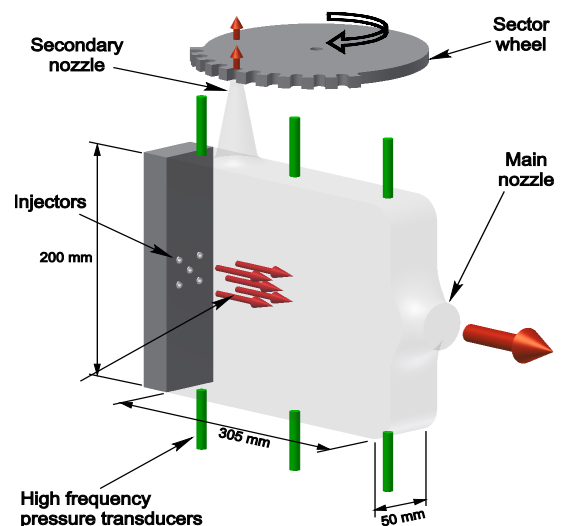


Figure 1. Illustration of combustion chamber BKH

Acoustic oscillations are imposed on the combustion chamber volume by modulation of mass flow through a secondary nozzle. The mass flow is modulated by passing a toothed wheel over the exit area of the nozzle (figure 1). For the investigation presented in this paper a 'sector wheel' was used. The sector wheel periodically modulates the exit of the secondary nozzle; each rotation has an excitation phase as the toothed section passes over the nozzle, and a relaxation phase where the non-toothed section passes and the nozzle is open. This allows the dynamic response of the system to be observed and the acoustic dissipation in the combustion chamber to be measured.

BKH is equipped with thermocouples, and low- and high-frequency pressure transducers. For this investigation, the dynamic pressure transducer located in the lower wall near to the injection plane (figure 1) was used to measure the acoustic pressure field in the combustion chamber.

To investigate flame-acoustic interaction, BKH is equipped with windows to directly observe the central combustion zone with high-speed optical diagnostics. For this investigation, one transparent and one 'dummy' window were installed. Two cameras, used in parallel via a dichroic mirror, were used to observe the flame zone. One camera recorded the visible spectrum with a resolution of $154 \mu\text{m}/\text{pixel}$ at 20,000 frames per second (fps), and a second, intensified camera was used to

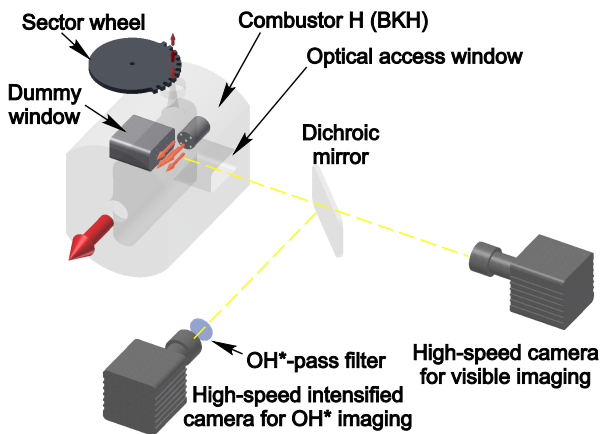


Figure 2. Optical diagnostic setup

capture filtered OH^* chemiluminescent emission with $446 \mu\text{m}/\text{pixel}$ at 30,000 fps. Figure 2 shows the layout of the optical setup.

The results presented in this paper come from a test conducted with cryogenic propellants. The hydrogen fuel was injected with a temperature of 48 K, and liquid oxygen with 120 K. The chamber was operated at a pressure of 40 bar with a ratio of oxidizer to fuel (ROF) of 6 in the primary flame region.

Results

Samples from the OH^* and visible emission spectrum imaging are presented in figure 3. The central combustion zone consists of a central injector which is surrounded by four others to provide representative conditions for the central element. Each image is a line of sight measurement of the central combustion zone. Due to the injector arrangement only three distinct jets are visible. In figure 4 the on the top is a visible image recording and on the bottom is an OH^* image recording in false colour.

In testing, the rotational speed of the sector wheel was set to target the first transverse (1T) resonance mode of the chamber, around 4100 Hz, which produced time varying acoustic excitation amplitudes. Figure 5 shows the oscillating amplitudes for the selected investigation period. The signal can be

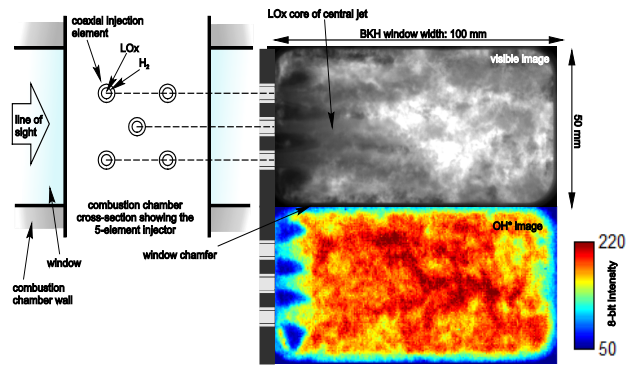


Figure 4. Instantaneous optical line of sight imaging results, visible spectrum (top) OH^* (bottom)

considered comprising two components; a low frequency oscillation, which corresponds to the sector wheel rotational frequency, and a high frequency signal with time varying amplitude, corresponding to the frequency imposed by the excitation wheel teeth. The low-frequency component and the amplitude of the high frequency components are overlaid on the raw signal in figure 4, which illustrates their relative phase.

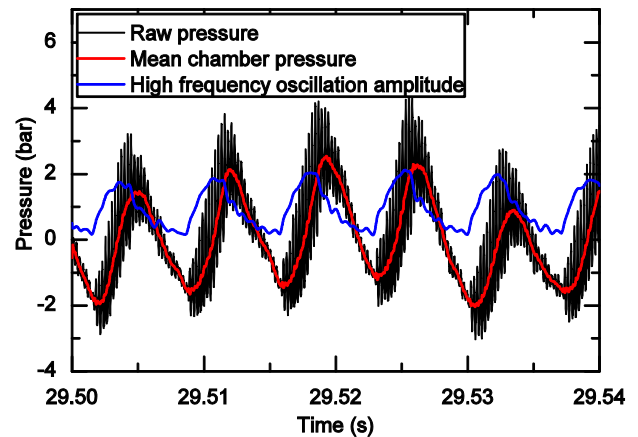


Figure 5. Acoustic pressure signal trace during excitation of the 1T mode

The amplitude of the high-frequency content leads that of the low-frequency content, or mean chamber pressure, by an average of 1.2ms or 4.9 high-frequency oscillations. At the start of an excitation phase, when the teeth modulate the nozzle flow with high frequency, the high-frequency amplitude rises sharply. With the characteristic lag, the mean chamber pressure begins to rise, in response to the partially reduced exhaust flow rate through the secondary nozzle. The end of the excitation phases correspond to the peaks of the high-frequency amplitude signal. The high-frequency amplitude decays with exponential character, which can be measured to assess acoustic damping in the combustion chamber. This is the subject of parallel analysis [10]. Again, there is a short delay after the excitation phase ends before mean combustion chamber pressure begins to normalise. This delay probably reflects the re-establishment of full flow through the open secondary nozzle and corresponding reduction in chamber pressure.

It is under this periodic acoustic forcing condition that the optical recordings were made. The central flame zone, visible in the optical images, is exposed to oscillations in transverse acoustic velocity during excitation of the 1T mode. The velocity antinode located in the central combustion zone is due to the pressure field distribution of the 1T mode.

The periodic excitation of the flame was observed in both the visible and OH^* recordings. A series of five images, taken across one period of relaxation and excitation, are presented in figure 6.

They are chosen according the cycle of mean image intensity, and are indicated on the intensity trace shown in figure 7.

Regions of high combustion and high density gradients are **regions of high intensity emission from combustion**

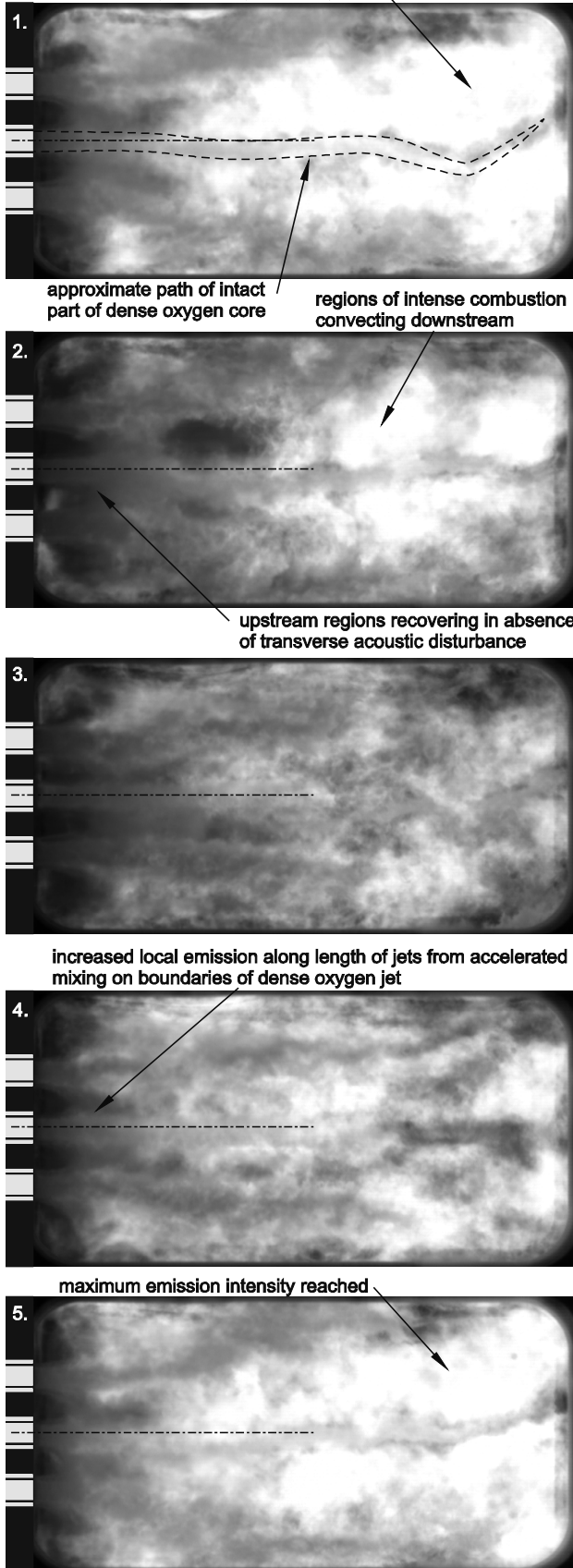


Figure 6. Image series from high speed visible imaging

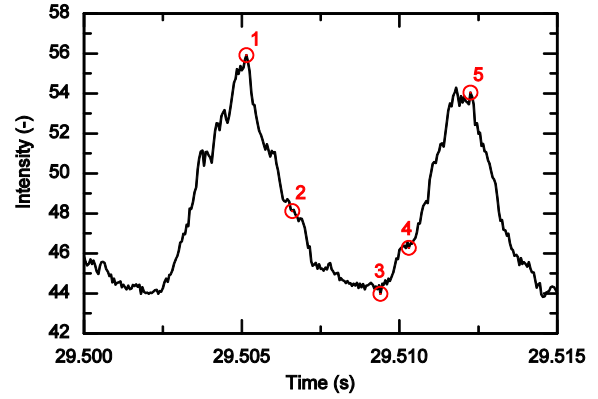


Figure 7. Trace of image mean intensity indicating selected time points for image sequence in figure 6

observable in visible spectrum imaging. This is different from OH* emission diagnostics which observe only areas of combustion regions associated with emission of the OH*. The areas of high intensity in the visible range are produced by combustion products such as water vapour not OH*. As such they do not represent the combustion zone directly. The images of low intensity represent areas of cold gas, with low levels of combustion. The comparison of visible and OH* emission results was given in figure 4. In the OH* image turbulent combustion is directly observable through emission of OH* and combustion can be seen to start in close proximity to the faceplate.

In figure 6 the location of combustion can be observed over a relaxation and excitation cycle. High emission intensity can be observed in figure 7 during periods of high acoustic amplitude (sequence images 1 and 5). This behaviour corresponds to the flame withdrawing toward the face plate which has previously been observed under conditions with high acoustic oscillation amplitudes [2]. As acoustic amplitude decreases during the relaxation phase (sequence image 2), regions of high intensity are carried downstream with the mean flow. Sequence image 3 is taken from a period with low acoustic oscillation amplitude. The image is darker with few regions of increased intensity from combustion products. During the excitation phase, on either side of the central liquid oxygen jet, local combustion at the contact point between the oxygen and hydrogen can be observed to migrate toward the injection plane (sequence images 3, 4 and 5). This is consistent with improved jet break up and propellant mixing due to the imposed transverse acoustic velocity [3].

The behaviour of the flame in the visible and OH* spectrum under periodic excitation was investigated by comparing the mean intensity fluctuations in each image (figure 8). The oscillation of the OH* emission leads that of the visible image

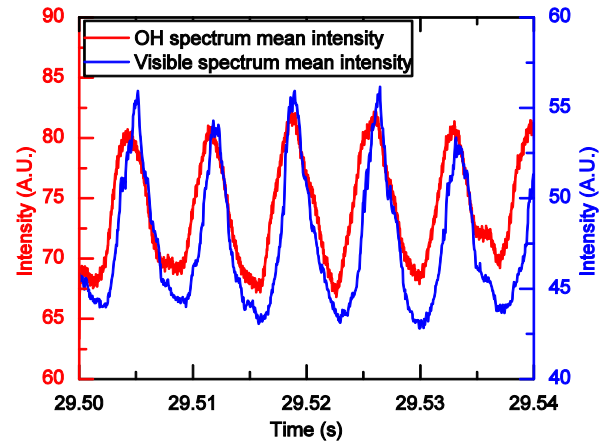


Figure 8. Mean frame intensities of image diagnostics

which can be partially attributed to the delay between instantaneous emission from oxygen-hydrogen reaction and sustained emission from thermally excited combustion products.

Figure 9 shows the power spectrum density (PSD) of acoustic energy at low frequencies for the mean OH* and visible intensities, and dynamic pressure. In figure 10 the PSD of the first tangential mode frequencies are presented. Both the OH* and visible mean intensities showed fluctuations at the first transverse mode resonance frequency. Additionally, non-linear coupling was observed between the wheel rotation frequency and the first tangential mode frequency for dynamic pressure, visible imaging and OH* imaging. Non-linear coupling of sector wheel rotation and Eigen mode frequencies has only been previously reported for dynamic pressure measurements [10].

It was not possible to compare the relative peak locations of the visible spectrum data with the dynamic pressure data due to a failure in the synchronisation signal. It is important to note, that a comparison between figures 5 and 8 can only be undertaken qualitatively in the time domain.

A further phenomenon of interest is observable in the high-speed visible image sequences. The dense jet of the liquid oxygen core is visible and its intact length and break up process relative to the acoustic amplitude can be qualitatively observed. Flame emission from combustion acts as the lighting source. The lighting source intensity varies both spatially and temporally which would make consistent measurement of intact length difficult. Such measurements are not attempted in the scope of this work.

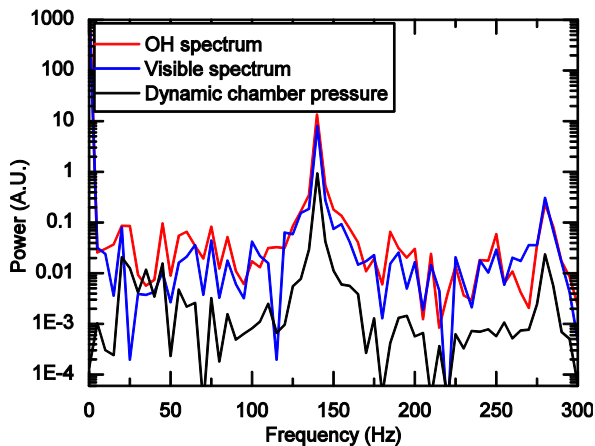


Figure 9. Low frequency content of high speed optical diagnostics and combustion chamber pressure

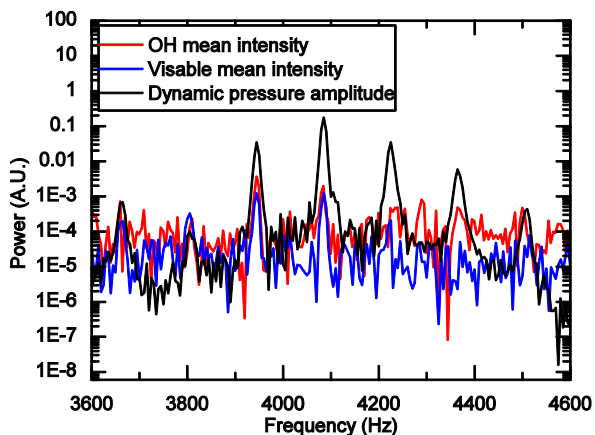


Figure 10. First transverse Eigen mode frequency content of high speed optical diagnostics and combustion chamber pressure

Conclusion

Investigations were carried out with high frequency optical diagnostics to observe flame-acoustic interaction. The acoustic mode investigated is the first transverse mode which has a velocity antinode located in the primary flame region. Use of visible spectrum diagnostic techniques allows the visualisation of both the dense gas phases and flame emission as a hybrid image. By cyclically varying the amplitude of acoustic excitation the response of the flame to rapidly changing acoustic conditions could be observed. Increased flame emission near to the face plate was observed for acoustic oscillations of high amplitude. Additionally, two localized combustion phenomena were observed. First, the convection of the combustion zones downstream with the relaxation of acoustic amplitude. Second, an increase in emission intensity at the mixing border between the dense oxygen core and the parallel cryogenic hydrogen was observed moving toward the injection plane for increasing acoustic amplitudes. This provides visual confirmation of increased mixing efficiency under combustion conditions close to the injection plane for high acoustic velocity amplitudes generated as a component of the first transverse mode.

References

- [1] Cheuret, F., *Instabilités thermo-acoustiques de combustion haute-fréquence dans les moteurs fusées*, Université de Provence Aix-Marseille, 2005.
- [2] Hardi, J. S., *Experimental investigation of high frequency combustion instability in cryogenic oxygen-hydrogen rocket engines*, The University of Adelaide, 2012.
- [3] Hardi, J.S., Beinke, S.K., Oswald, M., & Dally, B.B., Coupling of cryogenic oxygen-hydrogen flames to longitudinal and transverse acoustic instabilities, *J. Propul. Power*, 30, 2014, 991–1004.
- [4] Hardi, J. S., Gomez Martinez, H. C., Oswald, M., & Dally, B.B., LOx jet atomization under transverse acoustic oscillations, *J. Propul. Power*, 30, 2014, 337–349.
- [5] Harje, D. T. & Reardon F. H. (editors), *Liquid propellant rocket combustion instability*, National Aeronautics and Space Administration (NASA), 1972.
- [6] Méry, Y., Hakim, L., Scouflaire, P., Vingert, L., Ducruix, S., & Candel, S., Experimental Investigation of Cryogenic Flame Dynamics Under Transverse Acoustic Oscillations, *Comptes Rendus Mécanique*, 341, 2013, 100–109.
- [7] Rey C., Ducruix, S., Richecoeur, F., Scouflaire, P. & Candel, S., High Frequency Combustion Instabilities Associated with Collective Interactions in Liquid Propulsion, *40th AIAA/ASME/SAE/ASEE Joint Propulsion Conference & Exhibit*, 2004, pp. 1–13.
- [8] Richecoeur, F., *Expérimentations et simulations numériques des interactions entre modes acoustiques transverses et flammes cryotechniques*, École Centrale Paris, 2006.
- [9] Sliphorst, M., *High Frequency Combustion Instabilities of LOx/CH4 Spray Flames in Rocket Engine Combustion Chambers*, Technische Universiteit Delft, 2011.
- [10] Webster, S. C. L., Hardi, J. S., & Oswald, M., Experimental investigation of acoustic energy dissipation in a rectangular combustion chamber, in *5th European Conference for Aeronautics and Space Sciences*, 2013.
- [11] Yang, V. & Anderson, W. E. (editors), *Liquid rocket engine combustion instability*, American Institute of Aeronautics and Astronautics, 1995.